MATHEMATICAL BIOSCIENCES
AND ENGINEERING
Volume **4**, Number **3**, May **2007**

http://www.mbejournal.org/

pp. **431–456**

EFFECTS OF PREDATION EFFICIENCIES ON THE DYNAMICS OF A TRITROPHIC FOOD CHAIN

Maria Paola Cassinari

Dipartimento di Matematica, Università di Milano
via Saldini 50, 20133 Milano, Italy

Maria Groppi

Dipartimento di Matematica, Università di Parma
viale G. P. Usberti 53/A, 43100 Parma, Italy

Claudio Tebaldi

Dipartimento di Matematica, Politecnico di Torino
Corso Duca degli Abruzzi 24, 10129 Torino, Italy

(Communicated by Yang Kuang)

Abstract. In this paper the dynamics of a tritrophic food chain (resource, consumer, top predator) is investigated, with particular attention not only to equilibrium states but also to cyclic behaviours that the system may exhibit. The analysis is performed in terms of two bifurcation parameters, denoted by p and q, which measure the efficiencies of the interaction processes. The persistence of the system is discussed, characterizing in the (p, q) plane the regions of existence and stability of biologically significant steady states and those of existence of limit cycles. The bifurcations occurring are discussed, and their implications with reference to biological control problems are considered. Examples of the rich dynamics exhibited by the model, including a chaotic regime, are described.

1. **Introduction and model description.** Theoretical and experimental studies of population dynamics have received increasing interest in the last decades [2, 12, 18, 31], in particular for their applications to biological control problems. Biological control represents an important tool in constructing pest management strategy for protected plant production. It consists in rearing and releasing natural enemies (predators and parasites) that seek out and destroy other insects and mites that are considered pests; this practice allows regulating agricultural and forestry pests and weeds to densities below those of economic concern in a more natural way. In this context, the development of plausible mathematical models that reproduce and explain the observed dynamics of the interactions between natural enemies and harmful insects represents a challenging task, but also a valuable help in planning.

For a long time, the main attention was focused on the study of two trophic food chains, leading to a great variety of predator-prey models (see, for example, [2, 6, 22, 32]). More recently, various studies have been devoted to mathematical modelling of tritrophic food chains composed by prey (resource), predator (consumer of the

2000 *Mathematics Subject Classification.* 92D25, 34C23.
Key words and phrases. tritrophic system, stability, bifurcations, limit cycles.

resource) and top predator (natural enemy); just to mention a few, we recall here the paper of Freedman and So [9] on global stability and persistence of simple food chains, and the studies on bifurcations and chaotic dynamics performed by Hastings and coauthors [15, 21], by McCann and Yodzis [27, 28], by Kuznetsov and Rinaldi [24, 25], and by Boer et al. [3]. All these papers regard lumped-parameters prey-dependent models that can be described by a system of three balance equations having the following general form:

$$\begin{cases} \dfrac{dx}{dt} = rxg(x) - yb_1 f_1(px) \\ \dfrac{dy}{dt} = y[c_1 b_1 f_1(px) - m_1] - zb_2 f_2(qy) \\ \dfrac{dz}{dt} = z[c_2 b_2 f_2(qy) - m_2] \end{cases} \tag{1}$$

where $x(t)$, $y(t)$ and $z(t)$ are the biomass for spatial unit of resource, consumer and top predator, respectively. The functions g and $f_i, i = 1, 2$ determine the growth of the resource and the functional responses of predators to their prey, respectively. System (1) depends on some bioecological parameters: r is the maximum specific growth rate of the resource, b_1 and b_2 are the maximal specific predation rates and m_1 and m_2 are the specific loss rates (due to natural mortality and conversion processes) for consumer and top predator, respectively; c_1 and c_2 are conversion rates of prey into energy for its predator. The system depends also on two behavioural parameters $p, q > 0$ that measure the efficiencies of the predation processes. The function g in (1) may depend on x/k, where k denotes the carrying capacity of the resource, but it is possible to assume $k = 1$ via a suitable scaling, without loss of generality.

The bioecological parameters can be reasonably estimated from experimental data, while both the shapes of the functional responses and the values of the efficiencies of the interaction processes are very difficult to determine in realistic experimental set-up [19, 20]. Because of these difficulties, system (1) has been investigated in [5] by considering functional responses characterized only by some general properties; in addition, the behavioural parameters p and q, introduced in these trophic functions just as a measure of the efficiencies of the interaction processes, were assumed as control parameters in the analysis. In that general context, it was possible to investigate the existence conditions completely and the stability properties of the equilibrium states only partially; in particular, stability can be completely determined only for the noncoexistence equilibria.

In this paper we carry on the analysis started in [5] by fixing the functions g and f_i. According to the cited studies on simple tritrophic food chains, we assume a logistic growth for the resource and Holling-type-II trophic functions [2, 16] for the interaction processes, leading to the following expressions:

$$g(x) = 1 - x, \qquad f_i(s) = \frac{s}{1+s}, \quad i = 1, 2. \tag{2}$$

The regions in the (p, q) plane of existence and stability of nonnegative steady states, as well as their bifurcations, are here characterized, and in particular the ones leading to limit cycles are discussed. Bifurcation analysis of an equivalent formulation of system (1), with functions g and f_i as in (2), have been already performed in

[3, 8, 24, 25] with different choices of bifurcation parameters. In particular, the death rates m_1, m_2 have been used in [3, 25] for interpreting and forecasting the consequences of management actions, since these rates can be strongly influenced by harvesting the predators or by contaminating their environments. The carrying capacity k and the specific growth rate r have been used instead in [8, 24] to study the effect of enrichment of food chain systems. With these different choices of bifurcation parameters, the functional responses are completely fixed, and this could limit the applicability of the resulting analysis since, as already pointed out, the predation efficiencies which affect these functions are not easily determined.

Some results on the dynamics of the model by numerical investigation, using parameters related to p and q, have been presented in [27]; here we proceed in a more systematic way and specify and prove some of their results. In particular, the regions of existence and stability of coexistence equilibria will be analytically characterized.

We start our study by briefly recalling the main features of system (1). The state space is the nonnegative octant $\mathbb{R}^+_3$ and, following Freedman and So [9] and using comparison theory [14], it is possible to show that all solutions initiating in $\mathbb{R}^+_3$ are bounded and eventually enter the attracting set

$$\Omega = \left\{(x,y,z) \in \mathbb{R}^+_3 \mid \ 0 \le x \le 1,\, 0 \le x + \frac{y}{c_1} \le L_1,\, 0 \le x + \frac{y}{c_1} + \frac{z}{c_1 c_2} \le L_2\right\} \quad (3)$$

where $L_1 = 1 + \dfrac{r}{m_1}$, $L_2 = L_1 + \dfrac{r}{m_2} = 1 + \dfrac{r}{m_1} + \dfrac{r}{m_2}$.

We notice that on the invariant plane $z = 0$ in (1), the subsystem given by the first two equations can be regarded as the predator-prey system

$$\begin{cases} \dfrac{dx}{dt} = rxg(x) - yb_1 f(px) \\[2ex] \dfrac{dy}{dt} = y[c_1 b_1 f(px) - m_1] \end{cases} \quad (4)$$

where $x(t)$ and $y(t)$ represent the biomass for spatial unit of prey and predator.

The study of system (4) has been performed in general terms in [4] where a class of trophic functions depending on the ratio between the prey and a linear function of the predator abundance has been considered, aiming at analyzing the transition between prey-dependent and ratio-dependent models. In fact, the trophic functions used in predator-prey models in literature are mainly of two types: functions depending only on prey abundance (prey-dependent models [31]) and functions depending on the ratio between prey and predator abundances (ratio-dependent models [1]); some authors [10, 11] support the latter model on the basis of bioecological arguments based on experiments. The main difference is that only ratio-dependent models may predict the total collapse of chains [10, 17, 22, 32]. In addition, the functions f and g in [4] were characterized only by some general properties which are verified in particular by the choice (2). Here we detail the results of that analysis with reference to our specific case, namely the prey-dependent case with f and g as in (2).

- There exists an attracting and positively invariant set

$$\Omega^* = \left\{(x,y) \in \mathbb{R}^+_2 \mid \ 0 \le x \le 1,\, 0 \le x + \frac{y}{c_1} \le \left(1 + \frac{r}{m_1}\right)\right\}$$

which is the projection of Ω on the plane $z = 0$.

- The system has two noncoexistence equilibrium states $\mathsf{E}_0 = (0, 0)$ and $\mathsf{E}_1 = (1, 0)$ which exist for all $p > 0$. By investigating the Jacobian matrix evaluated at the equilibrium states, it results that the equilibrium E_0 is always a source, while E_1 is a sink for $0 < p < \chi_0 = f^{-1}\left(\frac{m_1}{c_1 b_1}\right)$, with $\frac{m_1}{c_1 b_1} < 1$, and a saddle otherwise.
- There exists a unique coexistence equilibrium $\mathsf{E}_2(p) = (x^*(p), y^*(p))$ for $p > \chi_0$. As regards its stability, there exists χ_1 such that E_2 is a sink for $\chi_0 < p < \chi_1$ and a source otherwise;. For $p = \chi_0(p)$ a transcritical bifurcation between E_1 and E_2 takes place and for $p = \chi_1$ a Hopf bifurcation of E_2 occurs.

Coming back to tritrophic system (1), its noncoexistence equilibrium states are related to these fixed points E_0, E_1, E_2. The existence conditions do not change, whereas the stability properties of these equilibria have to be investigated: this is done in section 2. In section 3 we determine the existence conditions and characterize the stability properties of coexistence equilibrium states. A bifurcation analysis in the (p, q) plane is presented in section 4, with particular attention to appearance of limit cycles because of Hopf bifurcations and bistability situations. In the appendix, in addition, we discuss the stability of the limit cycle which appears by Hopf bifurcation of $E_2(p)$. In section 5 we present some numerical simulations showing the different cyclic behaviours and an example of chaotic dynamics and discuss the biological meaning of such phenomena. Finally, some concluding remarks are reported in section 6.

2. **Existence and stability of noncoexistence equilibrium states.** We focus here on the noncoexistence equilibrium states (namely states with $z = 0$) of system (1). From (1) we have that if $\frac{m_i}{c_i b_i} \geq 1$, $i = 1, 2$, then asymptotically $y, z \to 0$; that is, both consumer and predator go to extinction. Thus, we will assume in the following

$$\frac{m_i}{c_i b_i} < 1 \tag{5}$$

and define

$$p_0 = f_1^{-1}\left(\frac{m_1}{c_1 b_1}\right) = \frac{m_1}{c_1 b_1 - m_1}, \qquad q_0 = f_2^{-1}\left(\frac{m_2}{c_2 b_2}\right) = \frac{m_2}{c_2 b_2 - m_2}. \tag{6}$$

It is also useful to define $\mu_i(s) = \frac{s f_i'(s)}{f_i(s)} = \frac{1}{1+s}, i = 1, 2$. It is easy to show that system (1) has two noncoexistence equilibrium states $E_0 = (0, 0, 0)$ (total extinction) and $E_1 = (1, 0, 0)$ (extinction of both consumer and top predator) and both exist for all values of p and q. In addition, if $p > p_0$ and for all values of q there exists a further noncoexistence state with $z = 0$ (extinction of top predator)

$$E_2(p) = (x^*(p), y^*(p), 0) = \left(\frac{p_0}{p}, \frac{r c_1}{m_1}\frac{p_0}{p}\left(1 - \frac{p_0}{p}\right), 0\right). \tag{7}$$

The noncoexistence equilibria of system (1) correspond to the equilibrium states of the two trophic levels system (4) when $z = 0$ is added as third component, in particular $E_2(p)$ corresponds to $\mathsf{E}_2(p)$ in system (4). The results about stability are summarized in the following theorem.

THEOREM 2.1. *Assume* (5) *and let*

$$\Gamma_0(p) = \frac{q_0}{y^*(p)}. \tag{8}$$

Then

1. *The equilibrium* E_0 *is a saddle point* $\forall\,(p,q) \in \mathbb{R}^+_2$*;*
2. *The equilibrium* E_1 *is a sink for* $0 < p < p_0$, $\forall q$ *and a saddle for* $p > p_0$, $\forall q$*;*
3. *When* $q < \Gamma_0(p)$ *there exists* $p_2 = 2p_0 + 1$ *such that* $E_2(p)$ *is a sink for* $p_0 < p < p_2$ *and a source for* $p > p_2$*. When* $q > \Gamma_0(p)$ *the equilibrium* $E_2(p)$ *is a source* $\forall p$*.*

Proof. Parts 1 and 2 easily follow by direct evaluation of the Jacobian matrices at the equilibrium states E_0 and E_1, which result respectively

$$J(E_0) = \operatorname{diag}(r, -m_1, -m_2), \qquad J(E_1) = \begin{pmatrix} -r & -b_1\dfrac{p}{1+p} & 0 \\ 0 & c_1 b_1 \dfrac{p}{1+p} - m_1 & 0 \\ 0 & 0 & -m_2 \end{pmatrix}. \tag{9}$$

Part 3 follows by considering the Jacobian matrix:

$$J(E_2(p)) = \begin{pmatrix} r\left(1 - 2\dfrac{p_0}{p}\right) - \dfrac{b_1 p y^*(p)}{(1+p_0)^2} & -\dfrac{m_1}{c_1} & 0 \\ b_1 c_1 \dfrac{p y^*(p)}{(1+p_0)^2} & 0 & -b_2 \dfrac{q y^*(p)}{1 + q y^*(p)} \\ 0 & 0 & b_2 c_2 \dfrac{q y^*(p)}{1 + q y^*(p)} - m_2 \end{pmatrix}. \tag{10}$$

It is important to notice that the minor of order two made up by the first two lines and columns

$$\begin{pmatrix} r\left(1 - 2\dfrac{p_0}{p}\right) - \dfrac{b_1 p y^*(p)}{(1+p_0)^2} & -\dfrac{m_1}{c_1} \\ b_1 c_1 \dfrac{p y^*(p)}{(1+p_0)^2} & 0 \end{pmatrix} \tag{11}$$

coincides with the Jacobian $J(\mathsf{E}_2)$ of the two trophic system (4) evaluated at the coexistence equilibrium state $\mathsf{E}_2(p) = (x^*(p), y^*(p))$. The eigenvalues of matrix (10) are then given by

$$\lambda_{1,2} = \frac{T(p) \pm \sqrt{T(p)^2 - 4D(p)}}{2}, \quad \lambda_3 = b_2 c_2 \frac{q y^*(p)}{1 + q y^*(p)} - m_2,$$

where $T(p)$ and $D(p)$ are respectively trace and determinant of the matrix (11). Direct calculations show that $Re(\lambda_{1,2}) < 0$ when $p_0 < p < p_2$ and λ_3 is always real and results negative only for $q < \Gamma_0(p)$. □

A more detailed description of the stability properties of $E_2(p)$ can be achieved by studying the trace and the determinant of matrix (11) and the sign of the function $\Delta(p) = T(p)^2 - 4D(p)$ that influence the nature of eigenvalues λ_1 and λ_2. Once z is set equal to zero and the sign of λ_3 is checked and found negative, namely $q < \Gamma_0(p)$, the results for the present case can be deduced from the analysis performed in [4] on system (4), having fixed g and f as in (2) and considering the prey-dependent case. In particular, it was shown that at the beginning the function $\Delta(p)$ is decreasing with respect to p and there exists a value $p_1 < p_2$ such

that $\Delta(p_1) = 0$. Afterwards, the function $\Delta(p)$ can decrease or increase depending on the set of bioecological parameters that influences the sign of the quantity Δ^*, defined as

$$\Delta^* = \lim_{p\to\infty} \Delta(p) = (1-\mu_{10})^2 - 4\frac{\mu_{10} m_1}{r},$$

with $\mu_{10} = \mu_1(p_0) = \dfrac{1}{1+p_0}$. When $\Delta^* > 0$, the function $\Delta(p)$ is definitely increasing and there exists another value $p_3 > p_2$ such that $\Delta(p_3) = 0$, then the equilibrium $E_2(p)$ admits again real eigenvalues. The results are then summarized in the following table, and it is remarkable that the local stability properties of $\mathsf{E}_2(p)$ in the two trophic level case spread to the whole region $p_0 < p < p_2$, $q < \Gamma_0(p)$ for the corresponding equilibrium state $E_2(p)$.

Table 1. Stability results for $E_2(p)$ in terms of p and q.

Conditions	Results
$q < \Gamma_0(p)$, $p_0 < p < p_2$	$E_2(p)$ sink
$q < \Gamma_0(p)$, $p > p_2$	$E_2(p)$ source
$q > \Gamma_0(p)$, $p_0 < p \le p_1 (\le p_2)$	$E_2(p)$ saddle
$q > \Gamma_0(p)$, $p > p_1$, $p \ne p_2$	$E_2(p)$ source

For $p = p_2$ the trace vanishes and $J(E_2)$ admits a pair of pure imaginary eigenvalues. It will be shown later that for $p = p_2$ a Hopf bifurcation, either supercritical or subcritical, of $E_2(p)$ occurs.

The global stability of the equilibrium $E_2(p)$ follows from a result of Chiu and Hsu [7], here adapted to our formulation.

THEOREM 2.2. *Let $(x(t), y(t), z(t))$ be a solution of system (1). If $p_0 \le p \le p_2$ and $q < \Gamma_0(p)$, then $(x(t), y(t), z(t)) \to (x^*(p), y^*(p), 0)$ as $t \to \infty$.*

For the proof, in [7] the following functional was considered:

$$V(x,y,z,p,q) = \frac{1}{c_1}\int_{y^*(p)}^{y} s^{\theta-1}(s - y^*(p))ds + y^\theta \int_{x^*(p)}^{x} \frac{f_1(p\xi) - m_1/(b_1c_1)}{f_1(p\xi)}\, d\xi + Cz. \tag{12}$$

Let the function $F : (0, x^*(p)) \cup (x^*(p), 1) \to \mathbb{R}$ be defined by

$$F(x,p) = \frac{\dfrac{y^*(p)}{c_1} - \dfrac{r}{b_1c_1p}(1-x)(1+px)}{\displaystyle\int_{x^*(p)}^{x} \frac{f_1(p\xi) - m_1/(b_1c_1)}{f_1(p\xi)}\, d\xi}$$

$$= \frac{\dfrac{y^*(p)}{c_1} - \dfrac{r}{b_1c_1p}(1-x)(1+px)}{\left(\dfrac{c_1b_1 - m_1}{c_1b_1}\right)\left[x - x^*(p) - x^*(p)\ln\left(\dfrac{x}{x^*(p)}\right)\right]}.$$

Then, $V(x, y, z, p, q)$ is a strictly Liapunov functional [26] if there exists $\theta > 0$ such that $\theta \geq F(x, p)$ for $0 < x < x^*(p)$ and $\theta \leq F(x, p)$ for $x^*(p) < x < 1$ and if C is chosen as

$$C = \frac{f_2(qy^*(p))}{c_1 c_2 q f_2'(qy^*(p))}(y^*(p))^{\theta-1}.$$

It was proven in ([7], theorem 3.1) that where $E_2(p)$ is locally stable, it is possible to verify the existence of θ which properly bounds $F(x, p)$.

3. **Existence and stability of coexistence equilibria.** The coexistence equilibrium states are strictly positive solutions of the following steady state equations:

$$rx(1-x) - b_1 y\frac{px}{1+px} = 0, \tag{13}$$

$$[c_1 b_1 \frac{px}{1+px} - m_1]y - b_2 z\frac{qy}{1+qy} = 0, \tag{14}$$

$$c_2 b_2 z\frac{qy}{1+qy} - m_2 z = 0. \tag{15}$$

From (13),(14) it follows that a necessary condition to have $z > 0$ is

$$x^*(p) = \frac{p_0}{p} < x < 1, \tag{16}$$

which implies $p > p_0$.

By direct calculations it follows that the coexistence equilibria are at most two and the expression of their components is reported in the following definition.

DEFINITION 3.1. *Let $E_3^{\pm}(p, q) = (x^{\pm}(p, q), y^{\pm}(p, q), z^{\pm}(p, q))$ denote two coexistence equilibrium states where*

$$x^{\pm}(p, q) = \frac{r(p-1)q \pm \sqrt{[rq(p+1)]^2 - 4rb_1 p^2 q_0 q}}{2rpq}, \tag{17}$$

$$y^{\pm}(p, q) = y(q) = \frac{q_0}{q}, \tag{18}$$

$$z^{\pm} = \frac{c_2 q_0}{m_2 q}\left[b_1 c_1 \frac{px^{\pm}}{1+px^{\pm}} - m_1\right]. \tag{19}$$

The existence regions of coexistence equilibrium states are characterized in the following theorem and are shown in figure 1.

THEOREM 3.1. *Assume* (5). *Let*

$$\Gamma_0(p) = \frac{q_0}{y^*(p)} = \frac{b_1 q_0}{r(1+p_0)}\frac{p^2}{p-p_0}, \qquad \gamma_0(p) = \frac{4b_1 q_0}{r}\frac{p^2}{(1+p)^2} \tag{20}$$

Then

- *for $p > p_2$, $\gamma_0(p) < q < \Gamma_0(p)$, there exist two positive coexistence equilibrium states $E_3^{\pm}(p, q)$;*
- *for $p > p_0$, $q > \Gamma_0(p)$, there exists a unique positive coexistence equilibrium state $E_3^{+}(p, q)$*

Proof. The second components $y^{\pm}(p, q)$ are positive for all $q > 0$, while from (17) it is easy to show that $x^{\pm}(p, q)$ are positive when $q > \gamma_0(p)$. The third components $z^{\pm}(p, q)$ are positive if and only if $x^{\pm} > p_0/p$. This condition guarantees of course also the positivity of the first component and leads to the following constraints:

- $x^-(p,q) > \dfrac{p_0}{p}$ in the region defined by
$$p > p_2, \qquad q < \Gamma_0(p),$$
- $x^+(p,q) > \dfrac{p_0}{p}$ in the region defined by
$$p < p_2,\ q > \Gamma_0(p) \qquad \text{and} \qquad p > p_2,\ q > \gamma_0(p).$$

Moreover, it is easy to show that $\gamma_0(p) \le \Gamma_0(p)$ for all $p > p_0$. All these conditions together prove the theorem. □

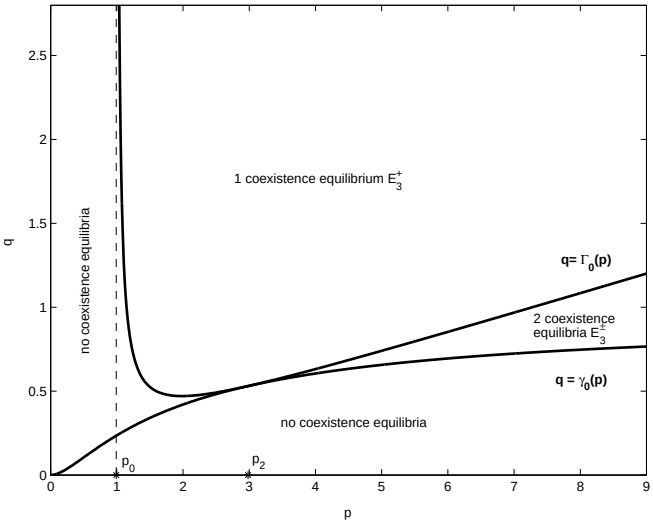

FIGURE 1. Existence regions of $E_3^\pm(p,q)$ in the (p,q) plane.

The stability of coexistence equilibria has been investigated via Routh-Hurwitz criterion that allows to study the stability properties without direct calculation of the eigenvalues of the Jacobian matrix.

THEOREM 3.2. *Assume* (5) *and the existence conditions of theorem 3.1. Then*

- *for $p_0 < p < p_2$ there exists a curve $q = \Sigma(p)$ such that $E_3^+(p,q)$ is locally asymptotically stable for*
$$\Gamma_0(p) \le q < \Sigma(p); \tag{21}$$
- *for $p > p_2$ there exists a curve $q = \gamma_0'(p)$ such that $E_3^+(p,q)$ is unstable for*
$$\gamma_0(p) \le q < \gamma_0'(p). \tag{22}$$

The equilibrium $E_3^-(p,q)$ is always unstable.

Proof. Let us consider the following Jacobian matrix of $E_3^\pm(p,q)$:

$$J(E_3^\pm) = \begin{pmatrix} r(1-2x^\pm) - \dfrac{b_1 q_0 p}{q(1+px^\pm)^2} & -b_1 \dfrac{px}{1+px^\pm} & 0 \\ \dfrac{c_1 b_1 q_0 p}{q(1+px^\pm)^2} & (1-\mu_{20})\left[c_1 b_1 \dfrac{px^\pm}{1+px^\pm} - m_1\right] & -\dfrac{m_2}{c_2} \\ 0 & \dfrac{c_2 b_2 q z^\pm}{(1+q_0)^2} & 0 \end{pmatrix} \tag{23}$$

where $\mu_{20} = \mu_2(q_0) = \dfrac{1}{1+q_0}$.
The Routh-Hurwitz criterion guarantees that all the eigenvalues of $J(E_3^{\pm}) = (j_{ik})$ have negative real part if and only if the following inequalities hold:

$$j_{11} + j_{22} = TrJ(E_3^{\pm}) < 0 \tag{24}$$

$$(j_{11} + j_{22})(j_{12}j_{21} - j_{11}j_{22}) + j_{22}j_{23}j_{32} > 0 \tag{25}$$

$$-j_{11}j_{23}j_{32} = DetJ(E_3^{\pm}) < 0. \tag{26}$$

The inequality (26) is never verified by $E_3^-(p,q)$ in the whole region of existence, since it results $j_{11}, j_{32} > 0$ and $j_{23} < 0$, and then it is always unstable. The same inequality is always true for $E_3^+(p,q)$, while expressions (24), (25) do not have a defined sign in the whole (p,q) plane. Let us consider the curve $q = \Gamma_0(p)$ for $p_0 < p < p_2$ on which $x^+ = p_0/p$ and $z^+ = 0$; then it results $j_{22} = 0$, $j_{11} = -r$, and the Routh-Hurwitz inequalities (24), (25), which simplify to

$$j_{11} < 0, \qquad j_{11}j_{12}j_{21} > 0, \tag{27}$$

are verified on such curve. Thus, by continuity, these inequalities together with the existence condition $q > \Gamma_0(p)$ define a stability region for $E_3^+(p,q)$ in the (p,q) plane bounded from below by $q = \Gamma_0(p)$ and from above by a curve $q = \Sigma(p)$; such curve can be pointwise approximated by checking where the Routh-Hurwitz conditions fail.

Now let us consider the curve $q = \gamma_0(p)$ for $p > p_2$ on which $x^+ = (p-1)/(2p)$; it results $j_{11} = 0$ and then the Routh-Hurwitz inequalities (24), (25) become on it:

$$j_{22} < 0, \qquad j_{22}(j_{12}j_{21} + j_{23}j_{32}) > 0. \tag{28}$$

Since $j_{22} > 0$ for $p > p_2$, these inequalities are never verified, and then on the curve $q = \gamma_0(p)$ the equilibrium $E_3^+(p,q)$ is unstable. Thus, by continuity there exists a region of instability bounded from below by $q = \gamma_0(p)$ and from above by a curve $q = \gamma_0'(p)$ that can be numerically approximated. □

REMARK 1. We notice that stability of the equilibrium $E_3^+(p,q)$ for $p \geq p_2$, $q \geq \Gamma_0(p)$ cannot be proven by using the previous technique, because on the curve $q = \Gamma_0(p)$ after p_2, the condition $x^+ = p_0/p$ fails and the Routh-Hurwitz inequalities do not have a defined sign. Anyway, it is possible to verify that the region of stability for $E_3^+(p,q)$ may extend also to $p \geq p_2$ depending on the set of fixed ecological parameters. In fact, the first of the Routh-Hurwitz conditions (24) concerns the sign of the trace of the Jacobian matrix $J(E_3^+)$. Since $Tr(J(E_3^+))$, which we indicate with $\tau(p,q)$, is null in correspondence of the point $A = (p_2, q_2 = \Gamma_0(p_2))$, the stability of E_3^+ for $p \geq p_2$ can be verified by checking the sign of $\dfrac{d}{dq}\tau(p_2,q)_{|q=q_2}$. If such sign is positive, then $\tau(p_2,q) > 0$ for $q > q_2$ and the equilibrium $E_3^+(p,q)$ becomes unstable for $p \geq p_2$, $q \geq \Gamma_0(p)$, since (24) is not fulfilled and we have $\Sigma(p_2) = \Gamma_0(p_2)$; on the contrary, if such derivative is negative, then (24) is verified and by continuity we get $\Sigma(p_2) > \Gamma_0(p_2)$; thus, it follows that there exists a region also for $p \geq p_2$ in which $E_3^+(p,q)$ remains stable above $\Gamma_0(p)$. By direct calculations we have

$$\frac{d}{dq}\tau(p_2,q) = C_0 + C_1\frac{d}{dq}x^+(p_2,q),$$

where the constants C_0 and C_1 depend only on the ecological parameters. By direct investigation, we find that $x^+(p_2,q)$ is an increasing function of q, $x^+(p_2,q_2) =$

$p_0/(1+2p_0)$ and $\lim_{q\to q_2^+} \frac{d}{dq}x^+(p_2,q) = +\infty$. Thus, the stability of the equilibrium $E_3^+(p,q)$ follows by the sign of the constant C_1. For our set of data (see table 1) it results $C_1 < 0$; then the equilibrium remains stable also for $p \geq p_2, q \geq \Gamma_0(p)$, as confirmed by the numerical simulations presented in the following. On the contrary, in [5] the different choice of biological parameters leads to a stability region for $E_3^+(p,q)$ which ends at A.

4. **Bifurcation analysis in the parameter space** (p,q)**.** In this section we discuss the bifurcations taking place when the boundary lines of the existence and stability regions of the equilibrium states in the (p,q) plane are crossed.

First of all, in figure 2 we report the curves in the (p,q) plane relevant to existence conditions and to changes in the stability properties of the equilibrium states. These curves divide the plane in five regions, whose boundaries are listed in the following legend. All curves are obtained analytically except for the curve Σ, which has been computed numerically. The trivial noncoexistence equilibrium state E_0 does not appear in the bifurcation analysis, because it is a saddle point independently of the parameters p and q. It means that the total collapse of the system is not allowed by our prey-dependent model (1), as already pointed out in the literature [10, 17]. In addition, negative equilibrium states will be considered, even if they have no ecological meaning, when they play some role in the comprehension of the bifurcations occurring between equilibria. The limit cycles exhibited by the system are discussed here only in relation to bifurcation of equilibria; their descriptions will be presented in the next section.

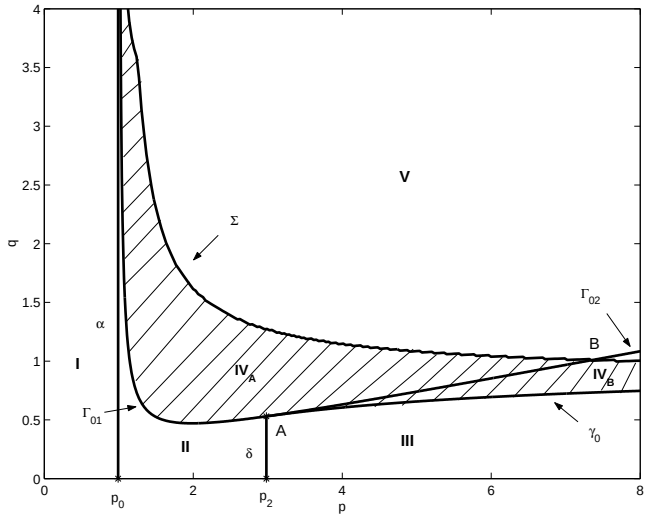

FIGURE 2. Existence and stability regions of the equilibrium states in the parameter space (p,q).

Legend:

- $A = (p_2, q_2)$: intersection of curves $q = \gamma_0(p)$ and $q = \Gamma_0(p)$;
- $B = (p_B, q_B)$: intersection of curves $q = \Gamma_0(p)$ and $q = \Sigma(p)$.
- α: line $p = p_0$;
- δ: line $p = p_2$ for $q < q_2$;
- γ_0: curve $q = \gamma_0(p)$ for $p > p_2$;

- Γ_{01}: curve $q = \Gamma_0(p)$ for $p_0 < p < p_2$;
- Γ_{02}: curve $q = \Gamma_0(p)$ for $p > p_2$;
- Σ: curve $q = \Sigma(p)$;

As pointed out in [29], many food chains belonging to the class vegetation-herbivore-carnivore (of interest in biological control) are characterized by diversified time responses, increasing along the chain from bottom to top. This leads to maximum specific growth rates r, $r_1 = c_1 b_1 - m_1$, $r_2 = c_2 b_2 - m_2$ in decreasing order, $r > r_1 > r_2$. In our simulations we use the parameter values collected in table 1, which have been deduced from the experimental data used by McCann and Yodzis [27] by suitable conversion of parameters and rates used in their formulation. The biological foundation of these values can be found in [33]. We notice that the scaling performed in [27] with respect to the carrying capacity k and the choice $r = 1$ yield dimensionless bioecological parameters. With this choice we obtain $r > r_1 > r_2$ and the following values for p_0, p_2, q_0 and q_2

$$p_0 = 0.99, \quad p_2 = 2.98, \quad q_0 = 0.25, \quad q_2 = 0.53.$$

Table 2. Values of dimensionless bioecological parameters used in the simulations.

r	b_1	b_2	m_1	m_2	c_1	c_2	$r_1 = c_1 b_1 - m_1$	$r_2 = c_2 b_2 - m_2$
1	0.94	0.11	0.4	0.01	0.85	0.45	0.399	0.0395

Comparison has been made with the values used by other authors, with reference to an equivalent formulation of system (1) (see for instance [25], table 1); we notice that almost all the parameters which are kept fixed in their studies become dependent on p and q. Thus, our variation of predation efficiencies induces variation in their parameters and, even if the corresponding values are of the same order of magnitude of ours, none of the cases presented there is exactly comparable with our results.

The existence of a stability region for the equilibrium $E_3^+(p, q)$ has been proven in theorem 3.2 for $p_0 < p < p_2$. According to the remark of the previous section, the numerical simulations show that, with the present choice of the ecological parameters, the Routh-Hurwitz conditions are satisfied also for values of p greater than p_2 and finally we obtain the stability region for $E_3^+(p, q)$ shaded in figure 2.

We now describe in detail the mathematical structure of the equilibria in the different regions of figure 2 and discuss the bifurcations across the boundaries, also considering the biological implications.

Region I $= \{(p, q) \in \mathbb{R}^2_+ : 0 < p < p_0\}$. In this region the noncoexistence equilibrium state E_1 is stable with three real negative eigenvalues. From a biological point of view, the stability of E_1, representing the total extinction of both individuals that attack the resource and their natural enemies, is the desired goal of an efficient biological control action. No other positive equilibrium states exist in this region. Therefore, persistence of the system cannot be reached here, (that is, coexistence is not allowed), because for $p < p_0$ (low consumer efficiency) the consumer of the resource can only decrease, driving the top predator toward extinction and all the trajectories toward E_1, which turns out to be globally stable.

Through α to region II. One real eigenvalue of E_1 becomes positive and the equilibrium state changes from stable to unstable, while $E_2(p)$ changes from negative to positive and becomes a sink. Along α the equilibrium states E_1 and $E_2(p)$ coalesce; they both have a simple null eigenvalue and exchange their stability. Then a *transcritical bifurcation* takes place at $p = p_0$.

Region II $= \{(p, q) \in \mathbb{R}^2_+ : p_0 < p < p_2,\ 0 < q < \Gamma_{01}\}$. The equilibrium E_1 is unstable, while $E_2(p)$ is locally stable in the whole region and, thanks to theorem 2.2, also globally stable. Coexistence equilibria do not exist in this region, which is characterized by low predation efficiencies for both consumer and top predator. From a biological point of view, the final outcome represents a stable coexistence of the resource and its consumer, in the absence of the biological control agent, so in this region the top predator cannot eradicate harmful individuals, because of its low efficiency.

Through Γ_{01} to region IV. The equilibrium state $E_2(p)$ changes from stable to unstable because a real eigenvalue changes from negative to positive. The coexistence equilibrium state $E_3^+(p, q)$ changes from negative to positive and becomes a sink. On the curve Γ_{01}, the equilibrium states $E_2(p)$ and $E_3^+(p, q)$ coalesce, with a simple eigenvalue which is zero. As a consequence, on the curve Γ_{01} an exchange of stability occurs between these two equilibrium states and a *transcritical bifurcation* takes place.

Through δ to region III. The equilibrium state $E_2(p)$ changes from stable to unstable. In the (x, y) plane a locally stable limit cycle O_{E_2} arises around $E_2(p)$. In fact, it is possible to prove the existence of a *supercritical Hopf bifurcation* for the equilibrium $E_2(p)$.

THEOREM 4.1. *Assume* (5). *Then for $p = p_2$, $q < \Gamma_0(p) = q_0/y^*(p)$ a supercritical Hopf bifurcation takes place for the equilibrium $E_2(p)$.*

Proof. Let us consider the Jacobian matrix (10). By direct calculation it follows that $T(p_2) = 0$, $D(p_2) > 0$ and in correspondence of the value $p = p_2$ the matrix has two pure imaginary eigenvalues $\lambda_{1,2} = \pm i\sqrt{D(p_2)}$ and no other eigenvalues with zero real parts. Moreover

$$\frac{d}{dp}\left(\Re e(\lambda_{1,2}(p))\right)_{|p=p_2} = \frac{r}{2}\frac{dT(p)}{dp}_{|p=p_2} = \frac{r}{2}\frac{p_0}{p_2^2} > 0.$$

Then, all the hypotheses of the Hopf theorem [13] are satisfied and a limit cycle for $p > p_2$ can be found; its stability is discussed in the appendix. All these conditions together prove the existence of a supercritical Hopf bifurcation for the equilibrium $E_2(p)$. □

Region III $= \{(p, q) \in \mathbb{R}^2_+ : p > p_2,\ 0 < q < \gamma_0 = 4b_1q_0p^2/r(1 + p)^2\}$. Both equilibrium states E_1 and $E_2(p)$ are unstable, and no coexistence equilibrium states exist in this region. Only the limit cycle O_{E_2} is locally stable, and the numerical simulations show that all the trajectories converge to the cycle. Then the final outcome in this region is the cyclic behaviour of the resource and its consumer, while the natural enemy goes to extinction without eradicating harmful individuals.

Through γ_0 to region IV. On this curve the coexistence equilibrium states $E_3^{\pm}(p,q)$ appear together with two complex eigenvalues with positive real part and a real null eigenvalue. Moreover, by increasing q close to γ_0, the real eigenvalue becomes negative for E_3^+ and positive for E_3^-. Thus a local *tangent bifurcation* for the equilibrium states $E_3^{\pm}(p,q)$ takes place on γ_0.

Region IV $= \{(p,q) \in \mathbb{R}^2_+ : p_0 < p < p_2,\, \Gamma_0(p) < q < \Sigma(p)\} \cup \{p > p_2,\, \gamma_0(p) < q < \Sigma(p)\}$.
In this region the noncoexistence equilibrium states E_1 and $E_2(p)$ are unstable in the whole region as well as $E_3^-(p,q)$, which exists only for $p > p_2$, $\gamma_0(p) < q < \Sigma$. For $p_0 < p < p_2$ the stability of the equilibrium $E_3^+(p,q)$ has been proven in theorem 3.2, while for $p > p_2$ may be investigated numerically by checking the inequalities (24)-(26) of the Routh-Hurwitz criterion. In particular, for values of q very close to $\gamma_0(p)$, two eigenvalues of $E_3^+(p,q)$ are complex with positive real part, and trajectories starting close to such equilibrium converge to the limit cycle O_{E_2}. By slightly increasing q, the complex eigenvalues become pure imaginary and then with negative real part. Thus, we have evidence of a *subcritical Hopf bifurcation* on a curve $\gamma_0'(p)$ very close to $\gamma_0(p)$, according to the second part of theorem 3.2. Such curves turn out to be very close to each other with the choice of parameters of table 1. From a biological point of view, in the region under consideration (but restricted to $\gamma_0'(p) < q < \Sigma(p)$ for $p > p_2$), stable coexistence of the resource, the consumer and the consumer's natural enemy can happen and this result could be useful if reached with low levels of harmful individuals.

Region IV can be further divided into regions IV_A and IV_B by considering the curve Γ_{02}. On this curve $E_2(p)$ and $E_3^-(p,q)$, both unstable, coalesce and then $E_3^-(p,q)$ becomes negative above this curve. Thus, on Γ_{02} a *transcritical bifurcation* of equilibria takes place.

Through Σ to region V. The coexistence equilibrium state $E_3^+(p,q)$ changes from stable to unstable, and on the curve Σ it has two pure imaginary eigenvalues and one strictly negative eigenvalue, respectively. The numerical simulations show that on this curve a *Hopf bifurcation* of $E_3^+(p,q)$ occurs; a limit cycle with all components oscillating between strictly positive values may be found above Σ and we have numerical evidence of the existence of a value $p_B > p_2$ such that the bifurcation is supercritical for $p < p_B$ and subcritical for $p > p_B$. The value p_B corresponds to the abscissa of the point B, intersection of Γ_{02} with Σ.

Region V $= \{(p,q) \in \mathbb{R}^2_+ : p > p_0,\, q > \Sigma\}$. No stable equilibrium states exist in this region and the extensive numerical simulations show the presence of stable limit cycles (see next section) and the possibility of chaos. In this region, it is possible to single out subregions in which the system is strongly persistent, (that is, the three components oscillate between some maximum and minimum values that are strictly positive), and then partial collapse of the system can be avoided.

Remark 2. It is interesting to discuss in more detail the bifurcation diagram near the point $A = (p_2, q_2)$. Such point has codimension two, since $J(E_2(p_2))$ has two pure imaginary eigenvalues and one zero eigenvalue. From this point, several bifurcation curves emerge and they are represented in figure 3. First of all, we notice that it is difficult to distinguish the curves γ_0 and γ_0' with our set of parameters.

In addition to the bifurcation curves for equilibria already discussed, we find the curve Θ, which represents a *transcritical bifurcation of limit cycles*. In fact, the curve δ above A is a subcritical Hopf bifurcation for the saddle $E_2(p)$: crossing δ above A from left to right, $E_2(p)$ becomes a repeller and a saddle limit cycle O_{E_2} appears on the (x, y) plane. This cycle becomes stable when the curve Θ is crossed and the hypothesis is a transcritical bifurcation with a positive saddle cycle as in [25], emerged by subcritical Hopf bifurcation of $E_3^+(p, q)$ across γ_0' in region IV.

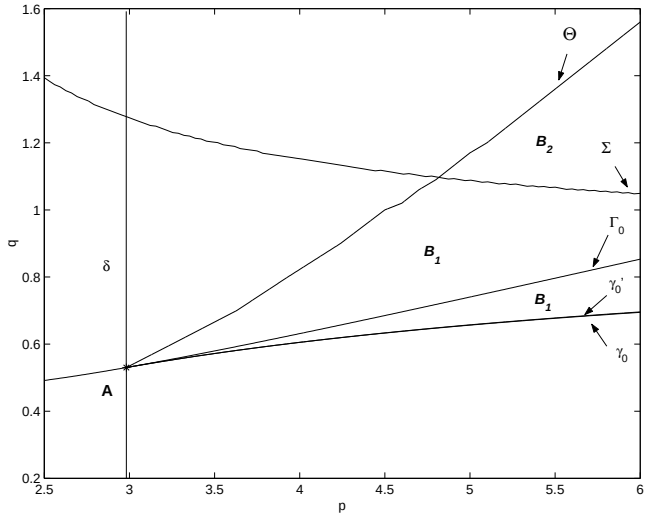

FIGURE 3. Bifurcation diagram around the codimension-two point A.

The cycle O_{E_2} is then stable in regions where other attractors are present. In particular, we obtain bistability between O_{E_2} and $E_3^+(p, q)$ in region B_1 (see figure 4 left) and bistability between O_{E_2} and a positive stable limit cycle O_{E_3} in region B_2 (see figure 4 right and section 5 for details on O_{E_3}). Our results essentially agree with those presented in [25], which were obtained in the parameter plane (m_1, m_2) by carrying out a parameter-dependent normal form analysis of the system near the codimension-two point A, and also with the subsequent numerical analysis of bistability phenomena presented in [3].

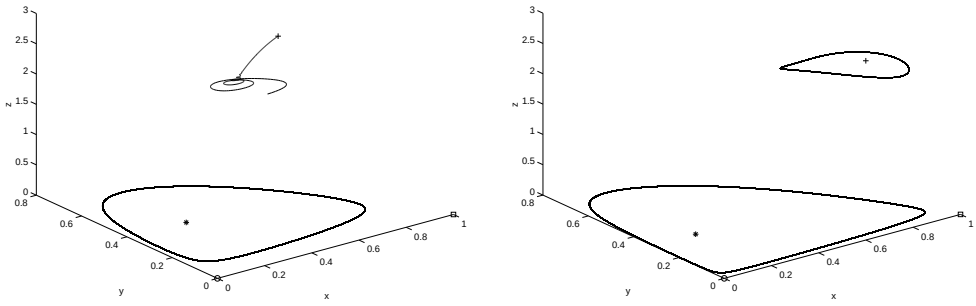

FIGURE 4. Bistability between the cycle O_{E_2} and the coexistence equilibrium state $E_3^+(p, q)$

($p = 4.1$, $q = 0.7$ in region B_1) (left) and between the cycles O_{E_2} and O_{E_3} ($p = 5.5$, $q = 1.2$ in region B_2) (right).

REMARK 3. The dependence of the asymptotic properties of the system on bioecological parameters different from p and q can be deduced from our analysis by drawing the curves giving the critical values in terms of r, m_i, c_i, b_i, $i = 1, 2$, in suitable subspaces. First of all, the carrying capacity k does not enter in our set, because from the beginning we have used scaled variables $x = \hat{x}/k$, $y = \hat{y}/k$, $z = \hat{z}/k$. This has led to predation efficiencies p and q which are measured in terms of k, and high values for such efficiencies may be the result of a high carrying capacity, namely productive environments.

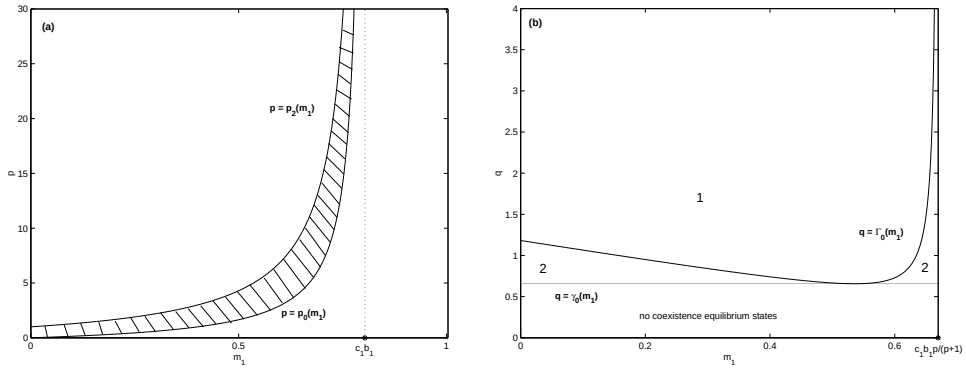

FIGURE 5. (a) Stability region (hatched) of $E_2(p)$ in the (m_1, p) plane; (b) regions of existence of the coexistence equilibrium states $E_3^{\pm}(p, q)$ in the (m_1, q) plane for $p = 5$. Other fixed parameters as in table 1, for which $c_1 b_1 = 0.8$ and $c_1 b_1 p/(p + 1) = 0.67$.

We now put in evidence the dependence of bifurcation values for p and q on the parameters m_1, m_2, r, which have been extensively used in the literature for bifurcation analyses.

The curve $p_0 = p_0(m_1)$ for $0 < m_1 < c_1 b_1$ is a portion of an increasing hyperbola, as well as $p_2 = p_2(m_1) = 1 + 2p_0(m_1)$. Both curves have a vertical asymptote at $m_1 = c_1 b_1$, and for $m_1 \geq c_1 b_1$ we get $\dot{y} < 0$ in system (1), and then both consumer and top predator go to extinction. The curve $q = \Gamma_0(m_1)$ is positive for $0 \leq m_1 < c_1 b_1 p/(p + 1) < c_1 b_1$ with a minimum at $m_1 = c_1 b_1 (p - 1)/(p + 1)$, and it bounds from below the region where the system admits only one coexistence equilibrium state. At the value $m_1 = c_1 b_1 p/(p + 1)$, which corresponds to $p = p_0$, the curve $q = \Gamma_0(m_1)$ has a vertical asymptote. The curve γ_0 instead does not depend on m_1, and then it is a line $q = \text{constant} > 0$ parallel to the axis m_1, which lies always below the curve $q = \Gamma_0(m_1)$ and it is tangent to it at its minimum $m_1 = c_1 b_1 (p - 1)/(p + 1)$, which corresponds to $p = p_2$. In the region between $\gamma_0(m_1)$ and $\Gamma_0(m_1)$, the system admits two coexistence equilibrium states.

With respect to m_2, both curves $q = \Gamma_0(m_2)$ and $q = \gamma_0(m_2)$, for $0 \leq m_2 < c_2 b_2$ and $p > p_0$, are portions of increasing hyperbolas which are tangent to each other at the origin of the (m_2, q) plane and such that $\gamma_0(m_2) \leq \Gamma_0(m_2)$. Moreover, both curves have a vertical asymptote at $m_2 = c_2 b_2$, and $\dot{z} < 0$ in system (1) for $m_2 \geq c_2 b_2$, and then top predator goes to extinction, so that no coexistence equilibria exist.

With respect to r and for a fixed $p > p_0$, the curve $q = \Gamma_0(r)$ is a branch of a

decreasing hyperbola for all $r > 0$, as well as $q = \gamma_0(r)$. Again, the curve $q = \gamma_0(r)$ is always below $q = \Gamma_0(r)$, and in the region bounded by the two curves there exist two coexistence equilibria.

To illustrate these results, we report the stability region for $E_2(p)$ in the (m_1, p) plane for a fixed $q < \min_p \Gamma_0(p)$ and the regions of existence of coexistence equilibrium states in the (m_1, q) plane in figure 5. The regions of existence of $E_3^{\pm}$ in the parameter planes (m_2, q) and (r, q), respectively, are then shown in figure 6. These last three figures are the analogues of figure 1 using different bifurcation parameters.

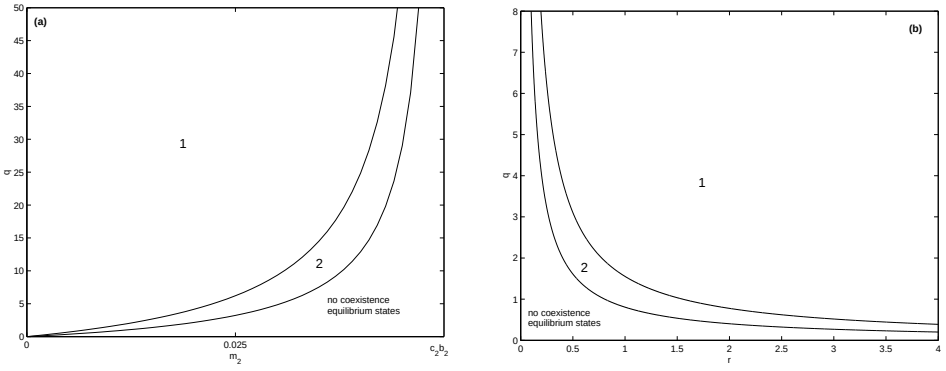

FIGURE 6. Regions of existence of the coexistence equilibrium states $E_3^{\pm}(p, q)$: (a) in the (m_2, q) plane for $p = 12$, (b) in the (r, q) plane for $p = 12$. Other fixed values as in table 1, for which $c_2 b_2 = 0.05$.

5. **Time-dependent behaviours: Limit cycles and an example of chaos.** Here we mainly investigate the temporal evolution exhibited by the system in the form of limit cycles, discussing their features from a biological point of view, and we show an example of chaotic behaviour. We start by considering the stable limit cycle O_{E_2}, arising from $E_2(p)$ in region III of figure 2, for a fixed value of q under the curve γ_0 and for increasing values of $p > p_2$. As pointed out in the previous section, in this region only the cycle O_{E_2}, lying in the plane $z = 0$, is locally stable and all the trajectories go toward such an attractor: the low level of efficiency q causes the extinction of the top predator. We notice that for $p > p_2$, $q < \gamma_0(p)$ both shape and period of the cycle O_{E_2} are not affected by the top predator efficiency q; therefore, the numerical simulations have been performed for the fixed value $q = 0.3$, representative of region III, without loss of generality. In all figures we show the behaviours after the initial transient, and we also report the positions of equilibria in the phase space, using the following symbols: '$\circ$' for E_0, '$\square$' for E_1, '$*$' for $E_2(p)$ and '$+$' for $E_3^+(p, q)$. The values for the period of the limit cycles are dimensionless, as a consequence of the choice $r = 1$. The following figures show the progressive increase of both period and amplitude of the cycle for increasing values of p (figs. 7–11). In particular, the period turns out to be a nearly linear function of the consumer efficiency.

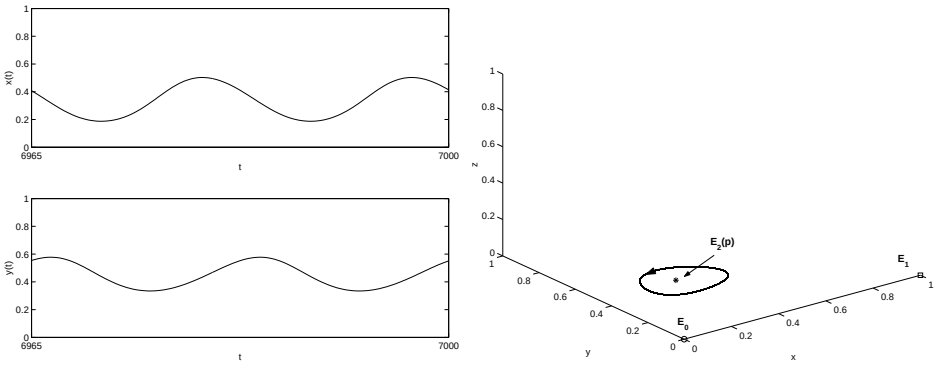

FIGURE 7. Temporal evolution of densities x, y for $p = 3.1$ (left) and the corresponding cycle O_{E_2} of period $T = 17.5$ (right).

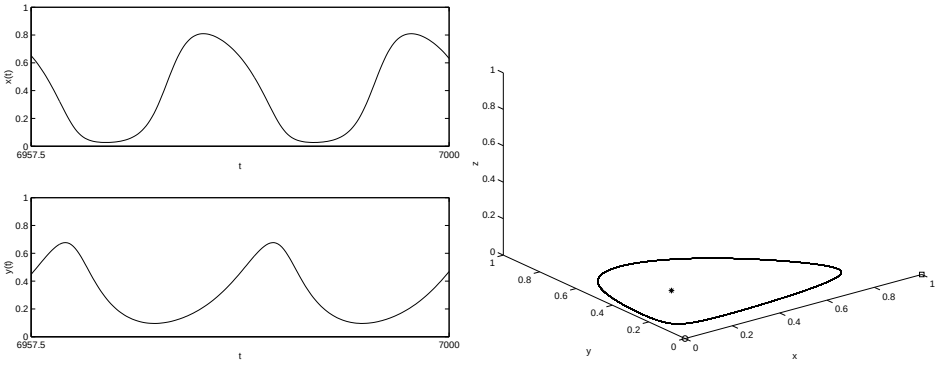

FIGURE 8. Temporal evolution of densities x, y for $p = 4.1$ (left) and the corresponding cycle O_{E_2} of period $T = 21.25$ (right).

By further increasing the value of the parameter p, the limit cycle O_{E_2} approaches the axes of the (x, y) plane, and, correspondingly, in the temporal evolutions the consumer remains at low levels between the maxima, which tend to be more and more peaked, while the resource alternates intervals in which it approaches its carrying capacity and intervals in which it is very low (figs. 9 and 10).

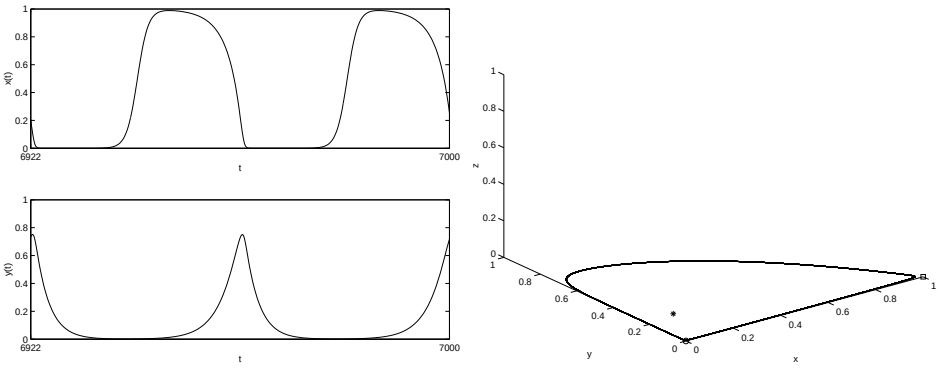

FIGURE 9. Temporal evolution of densities x, y for $p = 8$ (left) and the corresponding cycle O_{E_2} of period $T = 39$ (right).

All the previous figures show that there exists a threshold for the consumer density y that causes on one side the decrease of the resource when it is crossed from below and on the other side its growth when it is crossed from above. This value has been numerically estimated by taking the value of y in correspondence of the maximum of x and it results a decreasing function of p. Moreover, we point out that, for p large enough, O_{E_2} approaches the homoclinic cycle formed by the heteroclinic orbits connecting the saddle points E_0 and E_1, and correspondingly the temporal evolution shows longer and longer time intervals in which the system alternatively approaches the total extinction and the optimal condition (namely, resource close to carrying capacity and consumer close to zero) (see figure 10). The amplitude increase of the oscillation for the resource is an interesting phenomenon: while the progressive decrease of the minimum of resource for large values of the consumer efficiency could have been predicted, it is less obvious that a more efficient consumer may allow the resource to reach levels close to the carrying capacity of the system, for relatively larger and larger portions of the period. The result is a resource which, for almost half of the period, is close to its carrying capacity and for almost the other half is very low, with fast switches between the two cases. In the meantime, the consumer is at a very low level for most of the time and has bursts which cause the fast decrease of the resource.

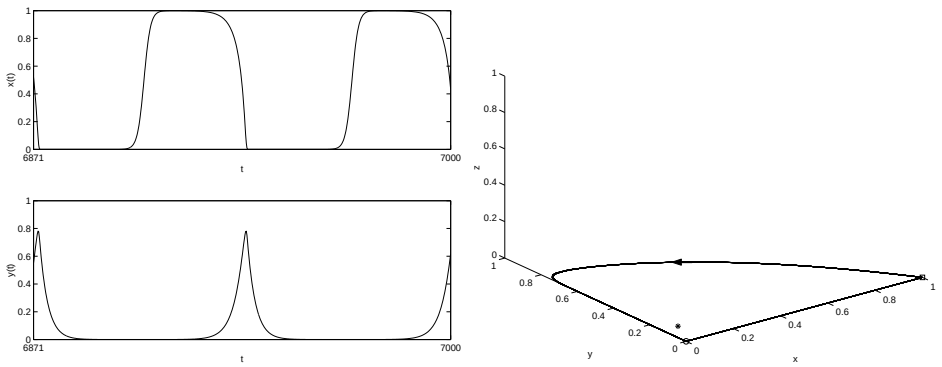

FIGURE 10. Temporal evolution of densities x, y for $p = 15$ (left) and the corresponding cycle O_{E_2} of period $T = 64.5$ (right).

Now we focus on the limit cycle O_{E_3}, which arises by Hopf bifurcation of $E_3^+(p, q)$ across Σ. This cycle corresponds to a persistence of the system, since its components oscillate between strictly positive values. We first follow its behaviour in region V of figure 2 for a fixed value of the parameter p in the interval $p_0 < p < p_2$ (low consumer efficiency) and for increasing values of q above the curve Σ. The following figures 11–14 are obtained for $p = 2.28$, representative of the region under study. The cycle increases its size and period and approaches the saddle point E_1, following the eigenspace tangent to its stable manifold ((x, z) plane), and then goes towards $E_2(p)$, following the direction of the unstable manifold of E_1. The temporal evolutions show that the oscillations of resource and consumer densities have nearly opposite phases, with a small delay between the maximum of y and the minimum of x, estimated as two to four time units for our set of parameters. Moreover, the figures show that there is now a threshold for the top predator density z, which causes the decay of the consumer and correspondingly the growth of the resource once it is crossed from below. This threshold can be estimated by taking the value

assumed by z when y reaches its maximum. It can be observed that the same threshold value for z also causes the reverse behaviour, once crossed from above; namely, the growth of the consumer and the decay of the resource. This mechanism is similar to the one observed for resource and consumer in the cycle O_{E_2}.

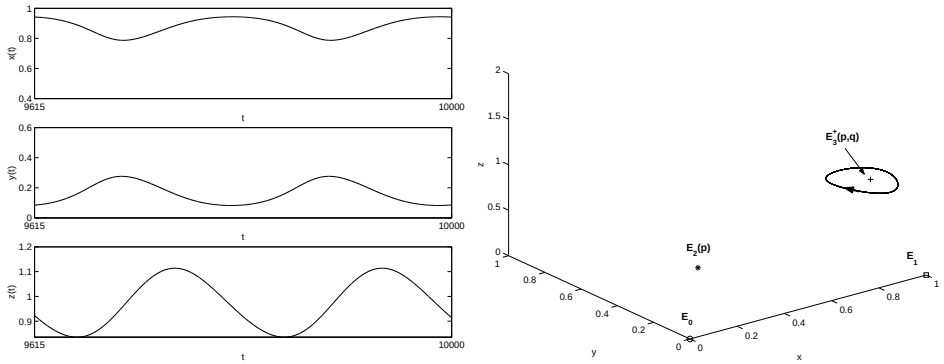

FIGURE 11. Temporal evolution of trophic levels for $q = 1.57$ (left) and the corresponding cycle O_{E_3} of period $T = 192.5$ (right).

Starting from figure 13, we see that when the first two components approach the equilibrium state $E_2(p)$, the corresponding temporal evolutions show the appearance of small scale oscillations. Moreover, for increasing q, the temporal evolutions show levels of the resource close to the carrying capacity of the system, and correspondingly very low consumer levels, for quite long time intervals (figs. 13–14). The figures denote also that higher values of the predation efficiency q cause a faster rise and a slower decay of z, that increase the length of the time interval in which the consumer remains at low levels. Such length is found to grow linearly with q. As a consequence, one could change favourably the system behaviour by introducing mechanisms of maintenance at suitable level for the top predator, with the aim to sustain the growth of the resource.

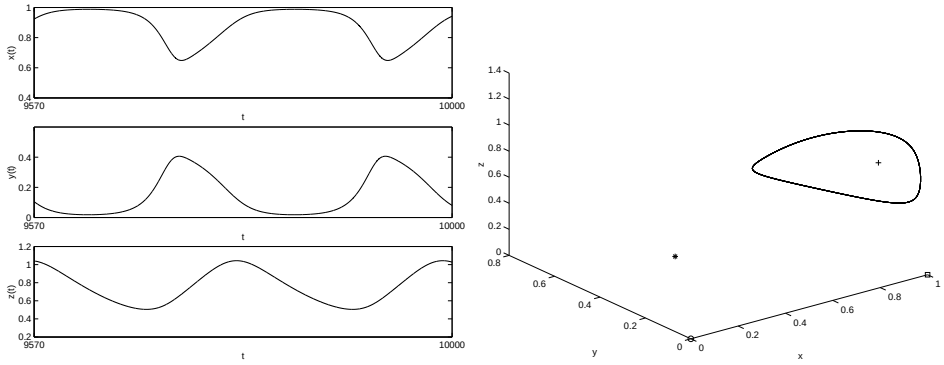

FIGURE 12. Temporal evolution of trophic levels for $q = 2$ (left) and the corresponding cycle O_{E_3} of period $T = 212$ (right).

We notice that in the chosen range of bifurcation parameter q, the system does not develop chaotic dynamics. We have also compared the limit cycles O_{E_2} and O_{E_3} for two different q's (on opposite sides with respect to Γ_0) and for the same

increasing p. The numerical results have shown that the oscillations in the x and y components are larger for the former than for the latter, and the period of O_{E_2} is always about one order of magnitude shorter than the period of O_{E_3}. Moreover, the two cycles show quite different behaviours: O_{E_3} presents changes in the topology and a period that slightly varies with p, while O_{E_2} increases both amplitude and period without essentially changing its shape.

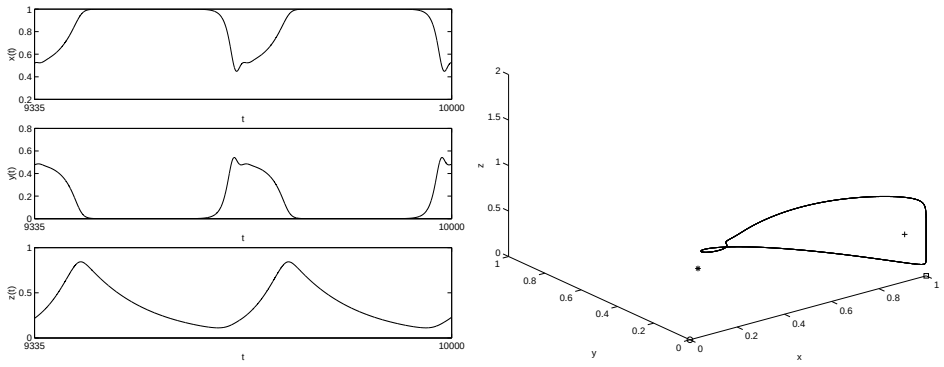

FIGURE 13. Temporal evolution of trophic levels for $q = 3.97$ (left) and the corresponding cycle O_{E_3} of period $T = 332.5$ (right).

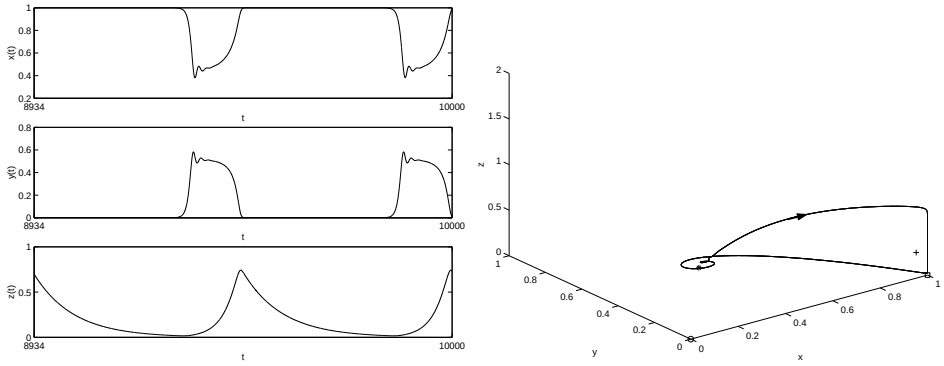

FIGURE 14. Temporal evolution of trophic levels for $q = 7.47$ (left) and the corresponding cycle O_{E_3} of period $T = 533$ (right).

Finally, we present the behaviour of the stable limit cycle O_{E_3} when a fixed large value of the consumer efficiency $p > p_2$ and increasing values of q above the curve Σ are considered; namely, in region V of figure 2 for p greater than p_2. The dynamics shown by the following figures have been obtained for the value $p = 4.98$, representative of the region in the (p, q) plane under study, and for different values of q. We start with $q = 1.11$, slightly above the curve Σ, and we find the cycle O_{E_3} reported in figure 15. Again, we can see that resource and consumer densities have nearly opposite phases, with a delay between the maximum of y and the minimum of x which varies again from two to four time units and, by increasing q, we can observe the increase of the cycle period (figs. 16–17). We notice that, with respect to the previous case, the higher efficiency p makes the consumer y more resistent to the actions of the top predator, and its functional response on resource x leads

to more complicated shapes of the cycle. This gives rise to more pronounced small-scale oscillations, especially in the first two trophic levels, in intervals following the minimum of x and the maximum of y, respectively. Moreover, for larger q it is still evident the presence of a threshold value for the top predator density z; crossing this value from above causes the fast growth of the consumer, and correspondingly the resource starts decreasing. Contrary to the situation observed for $p < p_2$, it is harder to estimate the threshold value for z which takes the system back to the optimal condition, because of the small-scale oscillations following the maximum of y and the minimum of x. We can observe the two behaviours obtained for lower or higher consumer efficiencies p by comparing figure 17 with figure 12, corresponding to the same top predator efficiency q. In both cases, after the top predator z has reached its maximum and starts decreasing, the consumer is decreasing and attains to a very low level until a threshold value for z, close to the minimum, is reached. Then, the consumer starts to grow again, monotonically in figure 12 and with small-scale oscillation in figure 17, since it is more difficult to fight the consumer when its efficiency is higher. Correspondingly, small-scale oscillations appear in the resource density after the phase when it is close to its carrying capacity. In addition, the values of top predator densities in the oscillations are larger in the case of higher consumer efficiency.

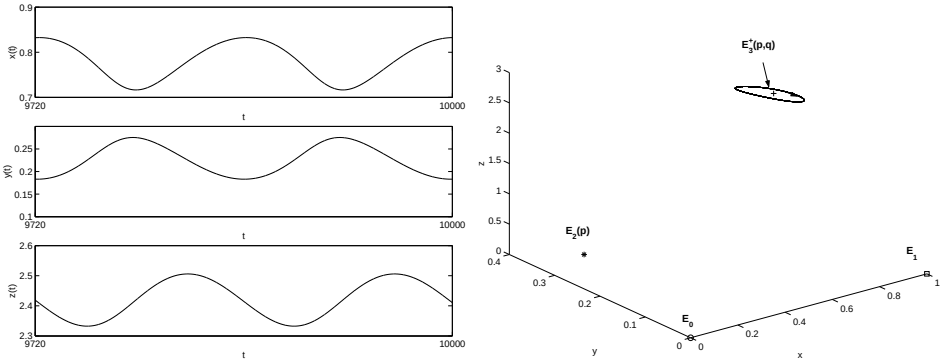

FIGURE 15. Temporal evolution of trophic levels for $q = 1.11$ (left) and the corresponding cycle O_{E_3} of period $T = 140$ (right).

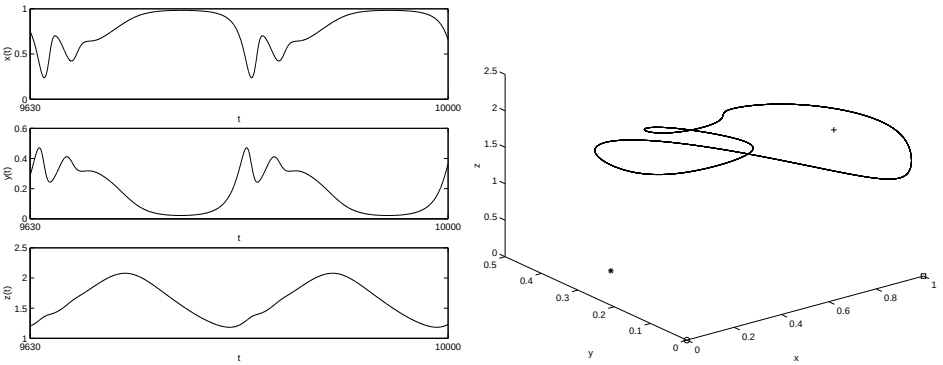

FIGURE 16. Temporal evolution of trophic levels for $q = 1.6$ (left) and the corresponding cycle O_{E_3} of period $T = 185$ (right).

The observed phenomenon of the appearance of high-frequency (small-scale) oscillations for the resource-consumer subsystem in the limit cycles O_{E_3} has been analyzed in [29]. It was detected in a class of tritrophic food chains, which our system belongs to, characterized by diversified time responses increasing from bottom to top. Using a singular perturbation approach, they showed that such systems can have low-frequency strictly positive cycles due to interactions between consumer and top-predator, while the interaction between resource and consumer can give rise to high-frequency oscillations. It was noticed that these periodic bursts of high-frequency oscillations develop, in particular, when consumer and top predator are fairly efficient and explicit conditions for their existence were derived; starting from these results, in our formulation a necessary condition turns out to be $p > p_2$, in agreement with our simulation.

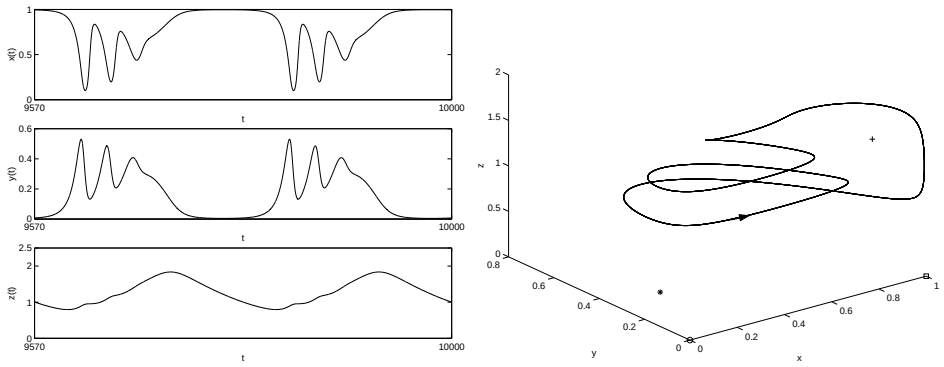

FIGURE 17. Temporal evolution of trophic levels for $q = 2$ (left) and the corresponding cycle O_{E_3} of period $T = 215$ (right).

As already shown in the literature [3, 15, 21, 24, 25, 28], food chain systems can develop chaotic dynamics in suitable ranges of bifurcation parameters, depending on the set of fixed bioecological rates. Such behaviours may explain irregular dynamics observed in many natural food chains (see discussion in [28]). The route to chaos was deeply investigated in [3, 21, 24, 25] using different bifurcation parameters. The first example of chaotic dynamics was shown by Hastings and Powell [15]; they found a strange attractor that strongly resembled a low-frequency cycle with bursts of high-frequency oscillations like the ones described in [29]. Klebanoff and Hastings [21] investigated the chaotic dynamics by deriving the normal form of a codimension-two bifurcation point, corresponding to point A in our formulation, and by showing that this normal form might imply chaos for small perturbation of the parameters. They numerically detected the presence of chaos by varying parameters corresponding to p and m_2. Later, it was noticed by Kuznetsov and Rinaldi in [25] that the origin of chaos cannot be associated to point A, but rather to more complex dynamical phenomena arising in regions far from the degenerate point. They showed that the transition to chaos, in a parameter plane corresponding to (m_1, m_2), involves a cascade of bifurcations and is related to the creation of a strange attractor like in [15]. With a different approach, in [3] a homoclinic bifurcation point was detected by Boer et al. and a region of chaotic coexistence, surrounding a region of extinction, was found by continuation techniques, in a subregion of the parameter plane (m_1, m_2). A systematic study of the chaotic regions was carried out by Kuznetsov et al. in [24] using r and k as bifurcation

parameters, beginning from the study of a codimension-two homoclinic bifurcation referred there to as Belyakov bifurcation.

In our formulation, the predation efficiencies p and q play the role of the main bifurcation parameters, since we are interested in discussing the phenomenology consequence of their variation, due to the fact that it is difficult to estimate them in any realistic experimental set-up. We have found strange attractors related to cycle O_{E_3} in region V, for consumer efficiency p high enough and increasing q. Here, we present in figure 18 the strange attractor, obtained for $q = 2.83$ and all other values as in figure 17, that resembles the surface of an upside-down tea cup. A similar attractor was also found by McCann and Yodzis in [27] using bifurcation parameters related to p and q, but, because of their choice, also changing the bioecological parameters corresponding to b_1, b_2 and m_2, fixed in our setting. By means of simulations and continuation, they started from the degenerate point corresponding to A but showed that chaos arises in a different region of the parameter space. In fact, in [28] the primary biological condition for chaos in this three trophic food chain was identified to be a productive environment, in the sense of high carrying capacity for the resource, that in our formulation can correspond to having sufficiently high predation efficiencies. In agreement with these conditions, the strange attractor presented in figure 18 has been obtained for p and q sufficiently high and far from the point A. However, a systematic investigation of transition to chaos for tritrophic food chains was presented in [25]. Even though their analysis was performed with a different set of bioecological parameters, our results are similar to the chaotic regime shown there.

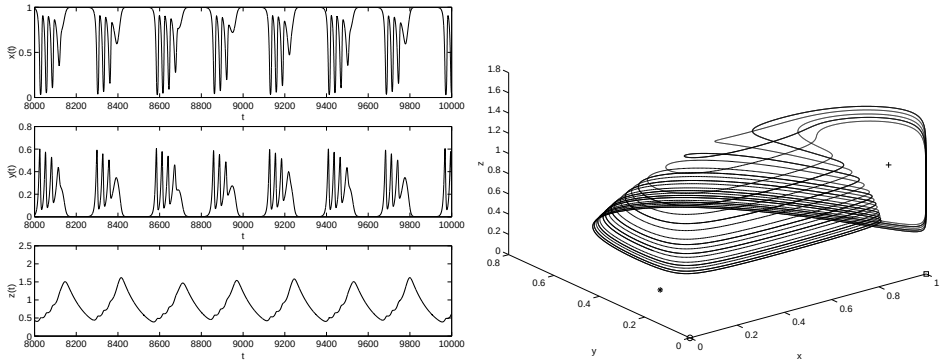

FIGURE 18. Temporal evolution of trophic levels for $q = 2.83$ (left) and the corresponding strange attractor in the phase space (right).

6. **Concluding remarks.** In this paper we have studied the prey-dependent food chain model resource-consumer-top predator, for which a bifurcation analysis has been carried out using the predation efficiencies p and q as control parameters, focusing on equilibria, limit cycles and with an example of chaotic behaviour. We have completely characterized equilibria and their regions of stability in the (p, q) plane, as well as the bifurcations at the boundaries between them and the appearance of limit cycles by Hopf bifurcation. We have proven the existence of several bifurcation curves, all analytically determined except two. We have also proven the stability of the limit cycle O_{E_2} in the plane $z = 0$, appearing by Hopf bifurcation of the equilibrium state E_2, representing the coexistence of resource and consumer in absence of the top predator. The resulting framework has been compared with

the existing literature on this subject. Our results give a contribution to clarify the role played by predation efficiencies in determining the fates of a tri-trophic food chain, and they allow to describe different observable dynamics in the (p, q) plane.

As for the system's persistence, with reference to figure 2 we summarize that the three trophic levels can coexist only in regions IV and V. Moreover, the coexistence is not guaranteed for all initial conditions in some subregions of IV and V. In fact, the limit cycle O_{E_2} (with $z = 0$) may be locally stable for $p > p_2$ and $q > \gamma_0(p)$ (see figure 3, regions B_1 and B_2 of bistability). The coexistence can occur as a stable equilibrium state or as a limit cycle and even as a strange attractor. We have analytically shown that the region of stability of the coexistence equilibrium state strongly depends on the values of the other bioecological parameters (see remark 1), and we have pointed out that such values also affect the position and the shape of the bifurcation curves (see remark 2), which may almost overlap as it happens to γ_0 and γ_0' in figure 3. Therefore, the dependence of critical values and bifurcation curves in terms of other biological parameters has been also investigated (see remark 3). The biological implications of the cyclic behaviours have been discussed, with reference to relevant features arising in the temporal evolutions when predation efficiencies are varied. The presence of chaotic attractors has been also pointed out, and reference has been made to previous literature on the subject.

In particular, the cyclic behaviours show interesting mechanisms in the interactions between the three trophic levels; for instance, it is possible to estimate values of predation efficiencies for which the system approaches the optimal conditions, namely high levels of resource and low levels of consumer, for quite long time intervals. It is also possible to estimate a threshold for the top predator density leading the system close to the optimal conditions. These results can be useful in the choice of the biological control strategy, since they may suggest characteristics of top predator, depending on the status of the resource and the level of consumer density, in order to regulate the pest according to the economic concerns.

7. **Appendix: Stability of limit cycle O_{E_2}.** The Hopf bifurcation of the equilibrium $E_2(p)$ at $p = p_2$ in the tritrophic system (1) gives rise to a limit cycle in the (x, y) plane. The stability of this cycle can be deduced from the attractivity properties of the limit cycle which appears by Hopf bifurcation of $\mathsf{E}_2(p)$ in the two trophic system (4). In [23] it was shown that for the prey-predator system (4) the cycle O_{E_2}, when exists, is globally attractive (except $\mathsf{E}_2(p)$) in the (x, y) plane. If we consider the noncoexistence equilibrium $E_2(p)$ for the tritrophic system (1), we obtain that, in correspondence of the Hopf bifurcation value $p = p_2$, the third eigenvalue λ_3 of $J(E_2)$ is real. Furthermore, it is possible to characterize the central manifold of E_2 as the (x, y) plane and to find that the projection on this plane of system (1), linearized around $E_2(p)$, coincides with the linearization around $\mathsf{E}_2(p)$ of the two trophic system (4). Consequently, the cycle O_{E_2}, which exists for $p > p_2$, will result stable for $q < \Gamma_0(p)$, where $\lambda_3 < 0$. The Hopf bifurcation of $E_2(p)$ will be supercritical for $p > p_2, q < \Gamma_0(p)$ and subcritical for $p > p_2, q > \Gamma_0(p)$.

In detail, let us consider the vectorial form $\dot{\mathbf{x}} = \mathbf{f}(\mathbf{x})$ of the system (1) and indicate with $J_f = (\mathsf{a}_{ij})$ the Jacobian matrix $J(E_2(p))$ (10). It is possible to find a linear transformation $\mathbf{x}' = B\mathbf{x}$ that maps $E_2(p)$ in itself, such that the new system

$\dot{\mathbf{x}}' = \mathbf{g}(\mathbf{x}')$ has a Jacobian matrix at $E_2(p)$ given by

$$J_g(\mathbf{x}') = BJ_f(\mathbf{x})B^{-1} = \begin{pmatrix} j_{11} & j_{12} & 0 \\ j_{21} & j_{22} & 0 \\ 0 & 0 & \mathsf{a}_{33} \end{pmatrix} \tag{29}$$

where a_{33} is the corresponding element in J_f, which represents also the third eigenvalue of the same matrix, and the entries j_{ik} are the same of the Jacobian $J(\mathsf{E}_2(p))$ of the two trophic case. In fact, let us consider the following matrix for the change of variables

$$B = \begin{pmatrix} 1 & 0 & \mathsf{b}_{13} \\ 0 & 1 & \mathsf{b}_{23} \\ 0 & 0 & 1 \end{pmatrix} \tag{30}$$

where

$$\mathsf{b}_{13} = -\frac{\mathsf{a}_{12}\mathsf{a}_{23}}{\mathsf{a}_{33}^2 - \mathsf{a}_{11}\mathsf{a}_{33} - \mathsf{a}_{12}\mathsf{a}_{21}}, \qquad \mathsf{b}_{23} = \frac{\mathsf{a}_{23}(\mathsf{a}_{11} - \mathsf{a}_{33})}{\mathsf{a}_{33}^2 - \mathsf{a}_{11}\mathsf{a}_{33} - \mathsf{a}_{12}\mathsf{a}_{21}}.$$

By substituting this transformation in (1) we obtain a system with a non-coexistence state $E_2'(p) = E_2(p)$ and the Jacobian matrix $J_g(\mathbf{x}')$ at E_2' turns out to be in the form (29).

Acknowledgments. We gratefully thank G. Buffoni for helpful suggestions and discussions. This work was performed in the frame of the activities sponsored by MIUR, by CNR, by GNFM and by the University of Parma (Italy).

References

[1] R. Arditi and L.R. Ginzburg, Coupling in predator-prey dynamics: ratio-dependence. J. Theor. Biol. 139 (1989) 311–326.
[2] A. D. Bazykin, Nonlinear Dynamics of Interacting Populations. Series of Nonlinear Science, Series A, Vol. 11. World Scientific, Singapore, 1998.
[3] M.P. Boer, B.W. Kooi and S.A.L.M Kooijman, Homoclinic and heteroclinic orbit to a cycle in a tri-trophic food chain. J. Math. Biol. 39 (1999) 19–38.
[4] G. Buffoni, M.P. Cassinari, M. Groppi and M. Serluca, Modelling of predator-prey trophic interactions. Part I. Two trophic levels. J. Math. Biol. 50 (2005) 713–732
[5] G. Buffoni, G. Di Cola and L. Garaventa, The local dynamics of a tri-trophic system. Ecol. Model. 138 (2001) 31–39.
[6] G. Buffoni and G. Gilioli, A lumped parameter model for acarine predator-prey population interactions. Ecol. Model. 170 (2003) 155–171.
[7] C.H. Chiu and S.B. Hsu, Extinction of top-predator in a three-level food-chain model. J. Math. Biol. 37 (1998) 372–380.
[8] O. De Feo and S. Rinaldi, Singular homoclinic bifurcations in tritrophic food chains. Math. Biosci. 148 (1998) 7–20.
[9] H.I. Freedman and J.W.H. So, Global stability and persistence of simple food chains. Math. Biosci. 76 (1985) 69–86.
[10] L.R. Ginzburg and H.R. Akçakaya, Consequences of ratio-dependent predation for steady-state properties of ecosystems. Ecology 73 (5) (1992) 1536–1543.
[11] A.P. Gutierrez, Physiological basis of ratio-dependent predator-prey theory: the metabolic pool model as a paradigm. Ecology 73 (5) (1992) 1552–1563.
[12] A.P. Gutierrez and Y. Wang, Applied population ecology: models for crop production and pest management. In: Norton, G.A., Holling, C.S. (Eds.), Pest Management. Pergamon, Oxford, 1976.
[13] J. Guckenheimer and P. Holmes, Nonlinear Oscillations, Dynamical Systems, and Bifurcations of Vector Fields. Springer-Verlag, New York, 1983.
[14] J.K. Hale, Ordinary Differential Equations. Wiley Interscience, New York, 1969.
[15] A. Hastings and T. Powell, Chaos in three-species food chain. Ecology 72(3) (1991) 896–903.

[16] C.S. Holling, The functional response of invertebrate predators to prey density. Mem. Ent. Soc. Can. 48 (1966) 3–86.
[17] S.B. Hsu, T.W. Hwang and Y. Kuang, A ratio–dependent food chain model and its applications to biological control. Math. Biosci. 181 (2003) 55–83.
[18] C.B. Huffaker, R.F. Luck and P.S. Messenger, The ecological basis of biological control. In: Huffaker, C.B., Messenger, P.S. (Eds), Theory and Practice of Biological Control. Academic, New York, 1976, 560–586.
[19] V. Hutson and R. Law, Permanent coexistence in general models of three interacting species. J. Math. Biol. 21 (1985) 285–298.
[20] P. Kareiva, The spatial dimension in pest-enemy interaction. In: Mackauer, M., Ehler, L.H., Roland, J. (Eds.), Critical Issues in Biological Control. Hants. Intercept, Andover, 1990, 213–227.
[21] A. Klebanoff and A. Hastings, Chaos in three-species food chain. J. Math. Biol. 32 (1993) 427–451.
[22] Y. Kuang and E. Beretta, Global qualitative analysis of a ratio–dependent predator–prey system. J. Math. Biol. 36 (1998) 389–486.
[23] Y. Kuang and H. I. Freedman, Uniqueness of limit cycles in Gause–type models of predator–prey systems. Math. Biosci. 88 (1988) 67–84.
[24] Yu. A. Kuznetsov, O. De Feo and S. Rinaldi, Belyakov homoclinic bifurcations in a tritrophic food chain model. SIAM. J. Appl. Math. 62 (2001) 462–487.
[25] Yu. A. Kuznetsov and S. Rinaldi, Remarks on food chain dynamics. Math. Biosci. 134 (1996) 1–33.
[26] J. La Salle and S. Lefschetz, Stability by Liapunov Direct Method. Academic Press, New York, 1967.
[27] K. McCann and P. Yodzis, Bifurcation structure of a three-species food chain model. Theor. Pop. Biol. 48 (1995) 93–125.
[28] K. McCann and P. Yodzis, Biological conditions for chaos in a three-species food chain. Ecology 75 (1994) 561–564.
[29] S. Muratori and S. Rinaldi, Low– and high–frequency oscillations in three–dimensional food chain systems. SIAM J. Appl. Math. 52 (1992) 1688–1706.
[30] L. Perko, Differential equations and dynamical systems. Springer-Verlag, New York, 1996.
[31] Y.M. Svirezhev and D.O. Logofet, Stability of Biological Communities. MIR Publishers, Moscow, 1983.
[32] D. Xiao and S. Ruan, Global dynamics of a ratio–dependent predator–prey system. J. Math. Biol. 43 (2001) 268–290.
[33] P. Yodzis and S. Innes, Body size and consumer–resource dynamics. American Naturalist 139 (1992) 1151–1175.

Received on July 19, 2006. Accepted on January 10, 2007.

E-mail address: cassinar@mat.unimi.it
E-mail address: maria.groppi@unipr.it
E-mail address: claudio.tebaldi@polito.it